Available online at www.sciencedirect.com
SCIENCE DIRECT
Journal of Geodynamics 41 (2006) 471–484
JOURNAL OF GEODYNAMICS
http://www.elsevier.com/locate/jog

Recent crustal deformation of İzmir, Western Anatolia and surrounding regions as deduced from repeated GPS measurements and strain field

Bahadır Aktuğ *, Ali Kılıçoğlu

Geodesy Department, General Command of Mapping, TR-06100 Ankara, Turkey

Received 24 May 2005; received in revised form 10 January 2006; accepted 27 January 2006

Abstract

To investigate contemporary neotectonic deformation in İzmir, Western Anatolia and in its neighborhood, a relatively dense Global Positioning System (GPS) monitoring network was established in 2001. Combination of three spatially dense GPS campaigns in 2001, 2003 and 2004 with temporally dense campaigns between 1992 and 2004 resulted in a combined velocity field representing active deformation rate in the region. We computed horizontal and vertical velocity fields with respect to Earth-centered, Earth-fixed ITRF2000, to Eurasia and to Anatolia as well.

The rates of principal and shear strains along with rigid-body rotation rates were derived from velocity field. Results show east–west shortening between Karaburun Peninsula and northern part of İzmir Bay together with the extension of İzmir Bay in accordance with general extension regime of Western Anatolia and Eastern Agea. East–west shortening and north–south extension of Karaburun Peninsula are closely related to right-lateral faulting and a clockwise rotation. There exists a block in the middle of the peninsula with a differential motion at a rate of 3–5 ± 1 mm/year and 5–6 ± 1 mm/year to the east and south, respectively.

As is in Western Anatolia, north–south extension is dominant in almost all parts of the region despite the fact that they exhibit significantly higher rates in the middle of the peninsula. Extensional rates along Tuzla Fault lying nearly perpendicular to İzmir Bay and in its west are maximum in the region with an extension rate of 300–500 ± 80–100 nanostrain/year and confirm its active state. Extensional rates in other parts of the region are at level of 50–150 nanostrain/year as expected in the other parts of Western Anatolia.

Keywords: Western Anatolia; GPS; İzmir Bay; Crustal deformation; Strain analysis; Repeated measurements

1. Introduction

Anatolia, as a natural laboratory for geosciences, involves various kinds of tectonic phenomena such as transform strike–slip faulting (North and East Anatolia Faults) continental collision and major thrust faulting (Bitlis-Zagros, Caucasus), continental escape (Anatolia), subduction (Nubia, Arabia), contraction (Caucasus, Marmara Sea), extension (Western Anatolia) and a variety of relatively small scale processes (Jackson and McKenzie, 1984; Taymaz et al., 1991; McClusky et al., 2000). A tectonic map of Anatolia and surrounding regions is shown in Fig. 1.

* Corresponding author. Tel.: +90 312 595 2258; fax: +90 312 320 1495.
E-mail address: baktug@hgk.mil.tr (B. Aktuğ).

0264-3707/$ – see front matter © 2006 Elsevier Ltd. All rights reserved.
doi:10.1016/j.jog.2006.01.004

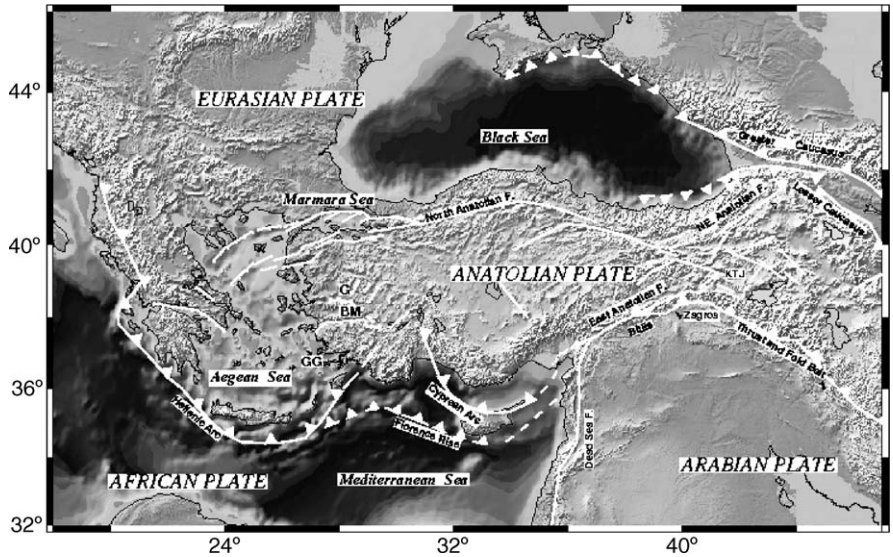

Fig. 1. Tectonic structure of Anatolia and surrounding regions (KTJ: Karliova Triple Junction; GG: Gulf of Gökova; G: Gediz Graben; BM:Büyük Menderes Graben).

Western Anatolia, characterized by N–S extension, parallel grabens and intervening horsts and associated normal faults, has been interest of many researchers (Jackson et al., 1992; Kissel et al., 1987; Lundgren et al., 1998; Kahle et al., 1998, 1999). Extension of Western Anatolia in N–S direction and increasing gradient of secular deformation rate toward Hellenic Arc have been shown by paleomagnetic, paleoseismological and geological evidence as well as regional seismological and Global Positioning System (GPS) studies for the present state deformation (Orbay et al.,

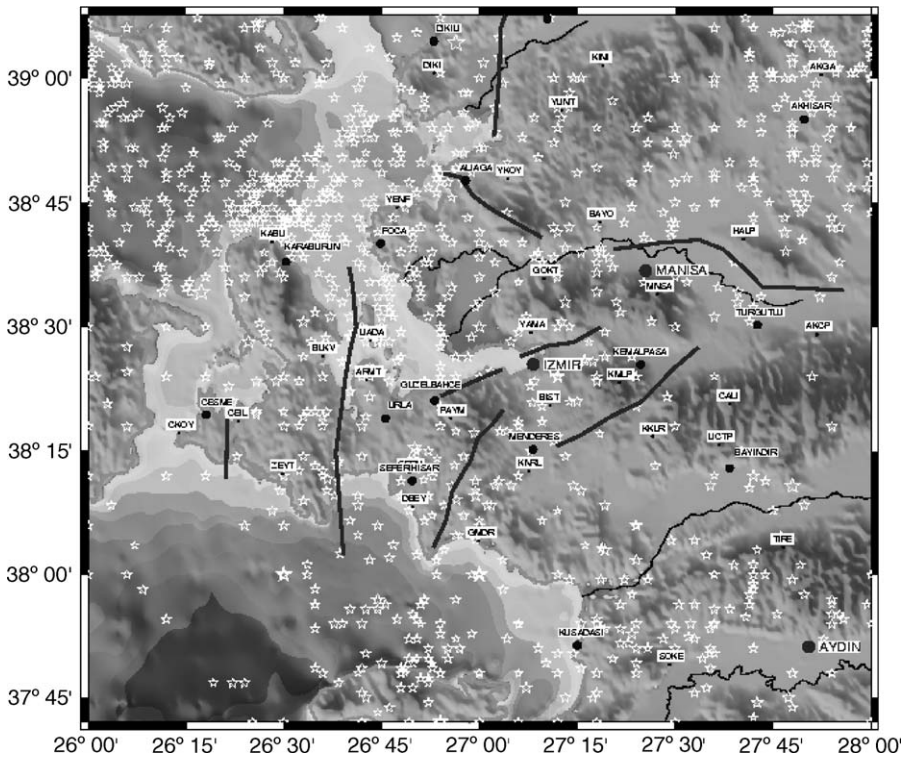

Fig. 2. Seismicity in İzmir and surroundings between 1900 and 2003 (earthquakes > Ms3.5).

2000; Ocakoğlu, 2004; Jackson et al., 1992; McClusky et al., 2000). Several projects were carried out in the region to investigate interseismic deformation through GPS measurements and they were mostly regional studies focusing on entire Western Anatolia and/or Agea (McClusky et al., 2000; Kahle et al., 1995, 2000; Aydan et al., 2000) and more recently by Nyst and Thatcher (2004). All these studies employed repeated GPS measurements to present neotectonic framework of Western Anatolia and they are particularly important in substantiating and quantifying the seismological evidence of extension regime (Eyidoğan, 1987). Rather than focusing on the entire Western Anatolia, this study also employs GPS data but with a focus on İzmir Bay and surrounding regions and with unprecedented temporal and spatial coverage.

İzmir, a metropolitan area of 2.5 million population, is believed to be subject to a potential catastrophic earthquake (Akıncı et al., 2000). According to seismological records of Kandilli Observatory and Earthquake Research Institute (KOERI), there have been historical earthquakes with intensity of 9–10 and a death toll of 15,000 people and tsunami were reported specifically for the earthquake in 1688 (http://www.koeri.boun.edu.tr). Although large earthquakes in the area have been reported, there has been no significant large-scale seismicity in the İzmir Bay for over a century (Akıncı et al., 2000; Ocakoğlu, 2004). Seismicity data of İzmir Bay and surrounding regions were taken from Kandilli Observatory and Earthquake Research Institute (http://www.koeri.boun.edu.tr) and are shown in Fig. 2.

A monitoring project was initiated in 2001, and a GPS monitoring network covering İzmir and surrounding region was established. The network consists of 37 sites, 22 of which were observed previously at least once between 1992 and 2001, while the rest were established within the project. Locations of the new sites were determined so as to provide a homogenous geographic coverage with particular emphasis on lineations of possible active faults (Tuzla Fault, Gülbahçe-Karaburun Fault and İzmir Fault) so as to control rotation of Karaburun Peninsula and extension of İzmir Bay as well. Location of GPS sites and major tectonic structures are given in Fig. 3.

GPS data were processed with Bernese Software V4.0 using standard IGS products (Rothacher and Mervart, 1996; Brockmann, 1996) and the campaign solutions were combined in ITRF2000 (Altamimi et al., 2002) using GLOBK Software (Herring, 1997). Daily repeatabilities of about 1–4 mm and 5–8 mm were obtained for horizontal

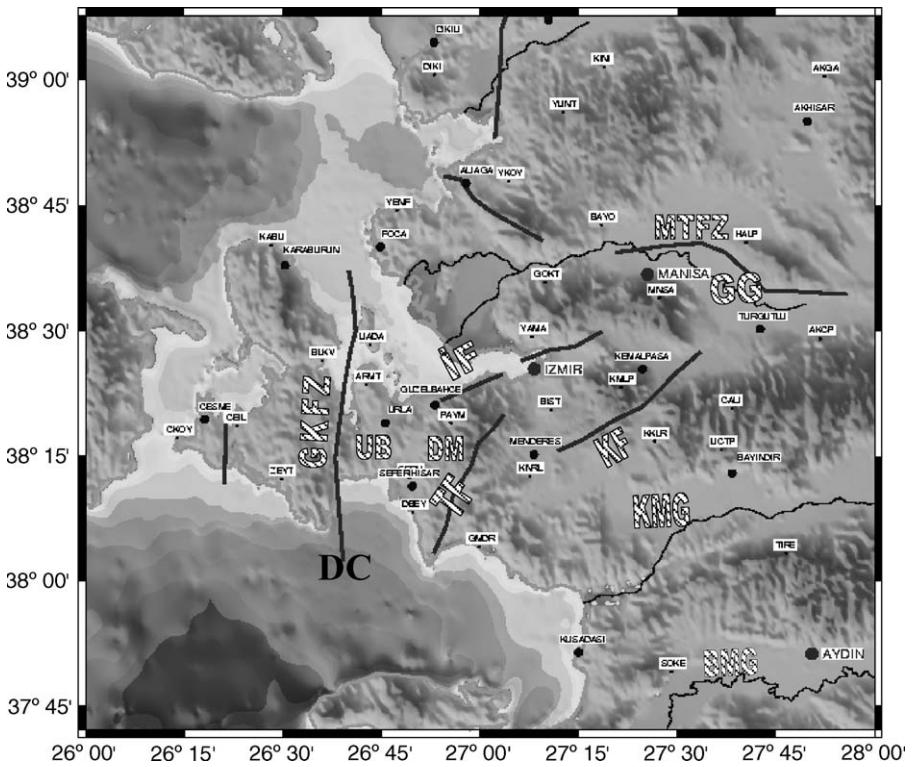

Fig. 3. GPS site locations and major tectonic structures in İzmir and surroundings (GKFZ: Gülbahçe-Karaburun Fault Zone; TF: Tuzla Fault; MTFZ: Manisa-Turgutlu Fault Zone; İF: İzmir Fault; KF: Kemalpaşa Fault; GG: Gediz Graben; KMG: Küçük Menderes Graben; BMG: Büyük Menderes Graben; DC: Doğanbey Cape; DM: Dikmen Mountain; UB: Urla Block).

and vertical components, respectively. Generic Mapping Tools were used for presenting graphics (Wessel and Smith, 1995).

Deformation rate of İzmir Bay and surrounding region is shown through relative velocity solutions with respect to No-Net-Rotation (NNR) frame of ITRF, to Eurasia (Eurasia-fixed frame) and Anatolia (Anatolia-fixed frame) as well as local combination of sites. Besides, a strain analysis method was employed to present deformation rate independent of reference frame, and to smooth velocities as well.

2. Tectonic setting

Tectonic framework of Mediterranean is dominated by collision of Arabian and African Plates with Eurasia (Jackson and McKenzie, 1984; Taymaz et al., 1991; McClusky et al., 2000). Westward extrusion of Anatolia along dextral North Anatolian Fault in the north and sinistral East Anatolian Fault in the south turns into a N–S extension in Western Anatolia. Subduction of Nubia in Hellenic Arc is the principal driving mechanism for N–S extension of Western Anatolia. Western Turkey in the south of 39.50N is extending in N–S with an upper bound rate of 20 mm/year, while Central and Eastern Anatolia are characterized by coherent and diffused deformation, respectively (Ayhan et al., 2003).

The only fault within the region of interest is Tuzla Fault, the activity of which has been agreed by the majority of researchers and taking place in Turkish Active Faults Map and it lies between Menderes and Doganbey Cape (Erdik et al., 1999; Şaroğlu et al., 1992). Taking place in a zone of three fault segments, Tuzla Fault forms the lineament trending NE–SW between Menderes Town and Doğanbey Cape. Geological observations reveal a right-lateral offset of 200–700 m at young river beds of Holocene age along Tuzla Fault as the latest earthquake, Ms6.0, 1992, shows a right-lateral focal mechanism (Ocakoğlu, 2004; Emre and Barka, 2000). Other potentially active faults are: Manisa Fault trending NW–SE between Manisa and Turgutlu with a length of about 25 km and Kemalpasa Fault of about 20 km length located on the southwestern side of E–W trending Gediz Graben. İzmir Fault, in the south of İzmir Gulf, which is two-segmented and E–W trending, and Gülbahçe-Karaburun Fault taking place in the Karaburun Peninsula are supposed to be predominantly strike–slip faults with a relatively small dip–slip component (Emre and Barka, 2000).

3. GPS observations and data handling

GPS observations in Turkey were initiated in late 1980s and have increasingly continued since then. Until the establishment of Turkish National Fundamental GPS Network (TNFGN), measurements were carried out with focus on North Anatolian Fault (NAF), East Anatolian Fault (EAF) and Marmara Region (Altiner et al., 1994; Straub and Kahle, 1995; Kahle et al., 1995; Kılıçoğlu, 1999; Ayhan et al., 2002b; McClusky et al., 2000). TNFGN, with over 600 homogenously distributed stations, forms the framework of geodynamical studies in Turkey (Ayhan et al., 2002a).

The monitoring network consists of 37 sites, 22 of which have interseismic velocities determined through observations between 1992 and 2001. More spatial coverage was obtained by three sequential surveys in 2001, 2003 and 2004. Distribution of GPS data span among campaigns is given in Table 1.

Data reduction and combination procedure was handled in a three step quasi-observation approach described by Dong et al. (1998) and Aktuğ (2004). First, individual GPS campaign observations from 1992 to 2003 were processed by using Bernese v4.0 software (Mervart, 1996; Rothacher and Mervart, 1996). For individual campaigns, loose solutions were produced through the combination of daily solutions by ADDNEQ as introduced in SINEX 1.1 format (Brockmann, 1996; Kılıçoğlu, 1999). Second, loosely constrained individual campaign solutions were coupled with weekly loose solutions of Center for Orbit Determination (CODE) (ftp://cddisa.gsfc.nasa.gov). This strategy provided the flexibility of defining reference frame as well as stability. Third, the reference frames (datum) for both coordinate and velocity estimates were defined by estimating 12-parameter transformation (3 translations, 3 rotations and their associated rates) to ITRF2000 coordinates of 17 IGS sites. Estimating 12 transformation parameters in an iterative least squares manner intrinsically involves minimizing misfit between solution coordinates and published ITRF2000 coordinates. Details of Helmert Method and transformation can be found in Altamimi et al. (2002).

Selection of sites for reference frame definition of both coordinates and velocities was made based on site history, long-term repeatability, geographic coverage of the region and availability in pre-processed regional solutions. Selected groups of sites according to criteria mentioned above are those defined as stable by Altamimi et al. (2002) and McClusky et al. (2000) and used by those studies for reference frame definition. The selected IGS sites and their velocities in local system are given in Table 2. Combination of loose campaign solutions (quasi-observations) was implemented

Table 1
Observation spans of GPS sites between 1992 and 2004

No.	Site	1992	1992	1993	1994	1994	1994	1996	1997	1997	1998	2000	2001	2002	2003	2004
1	ARMT											×	×		×	×
2	BAYO	×	×	×	×				×	×	×	×	×			×
3	BIST											×	×		×	×
4	BLKV												×		×	×
5	CALI											×	×		×	×
6	CEIL	×	×	×	×		×	×	×	×	×	×	×		×	×
7	CKOY												×		×	×
8	DBEY												×		×	×
9	DIKI	×				×			×				×		×	×
10	GMDR												×		×	×
11	KABU								×				×		×	×
12	KKLR												×		×	×
13	KMLP											×	×			×
14	KNRL												×		×	×
15	MNSA											×	×		×	×
16	PAYM												×		×	×
17	SFRH								×				×		×	×
18	UADA												×		×	×
19	YAMA	×	×	×	×					×			×		×	×
20	YENF	×	×	×	×				×	×		×	×		×	×
21	YKOY												×		×	×
22	YUNT												×		×	×
23	ZEYT												×		×	×
24	OZDE				×			×			×			×		×
25	AKCP	×		×	×				×							
26	AKGA	×	×	×	×						×				×	
27	AVCI	×		×	×				×							
28	AYKA	×			×			×	×		×	×			×	
29	CAKI	×		×	×				×							
30	DOGA	×		×	×				×	×						
31	GOKT	×		×	×				×							
32	HALP	×		×	×				×							
33	KINI	×			×			×			×					
34	KOB1								×							
35	SOKE	×		×	×			×								
36	TIRE	×		×	×				×							
37	UCTP								×					×		

in a Kalman filter approach using GLOBK software (Herring, 1997). Post-fit root-mean-square (RMS) of 17 stations was found to be 1.8 mm and 0.4 mm/year for coordinates and velocities, respectively. Taking the data interval spanning 12 years and number of sites used for reference frame definition into consideration, post-fit RMS is indicative of a consistent reference frame definition both for coordinates and velocities. Horizontal velocities with respect to ITRF2000 are shown in Fig. 4 and given in Table 3.

For a Eurasia-fixed frame, residual velocities of 17 IGS sites were obtained by differentiating ITRF2000 and Eurasia plate velocities as given in Eq. (1). The corresponding plate velocities for sites were computed from rotation pole of Eurasia in Altamimi et al. (2002) and given in Table 4. Then a Eurasia-fixed frame is realized using the stabilization (transformation) strategy described above with the residual velocities of 17 sites. Post-fit RMS of 17 stations was found to be 1.8 mm and 0.5 mm/year for coordinates and velocities, respectively. Velocities with respect to Eurasia are shown in Fig. 5a.

$$v_r = \hat{v}_{ITRF2000} - \hat{v}_{PLATE} \quad (1)$$

Velocities with respect to rigid part of Anatolia were obtained by removing the effect of rigid-body rotation of Anatolian Plate from Eurasia-fixed velocities of sites as described by Aktuğ (2003). Anatolia–Eurasia pole representing this

Table 2
IGS sites used for ITRF2000 realization

No.	Site	Longitude (°)	Latitude (°)	No. of epochs	First epoch	Last epoch	Interval (year)	v_N (mm)	v_E (mm)	v_U (mm)
1	BOR1	17.0735	52.2770	55	1996.73	2004.29	7.56	0.0137	0.0204	−0.0011
2	BRUS	4.3592	50.7978	55	1996.73	2004.29	7.56	0.0143	0.0181	0.0006
3	GOPE	14.7856	49.9137	41	1997.62	2004.29	6.67	0.0142	0.0206	−0.0011
4	GRAZ	15.4935	47.0671	61	1992.69	2004.29	11.60	0.0145	0.0221	−0.0023
5	JOZE	21.0315	52.0973	51	1996.73	2003.54	6.81	0.0133	0.0216	−0.0010
6	KIT3	66.8854	39.1348	52	1996.73	2004.29	7.56	0.0041	0.0280	−0.0015
7	KOSG	5.8096	52.1784	44	1996.73	2002.91	6.18	0.0153	0.0178	0.0007
8	MATE	16.7045	40.6491	67	1992.67	2004.29	11.62	0.0181	0.0237	−0.0010
9	ONSA	11.9255	57.3953	65	1992.67	2004.29	11.62	0.0136	0.0172	0.0026
10	PENC	19.2815	47.7896	45	1997.40	2004.29	6.88	0.0127	0.0226	−0.0004
11	POL2	74.6943	42.6798	46	1996.73	2004.29	7.56	0.0028	0.0278	0.0000
12	POTS	13.0661	52.3793	55	1996.73	2004.29	7.56	0.0142	0.0193	−0.0013
13	TRO1	18.9396	69.6627	31	2000.46	2004.29	3.83	0.0145	0.0139	0.0026
14	VILL	356.0480	40.4436	50	1997.62	2004.29	6.67	0.0157	0.0193	−0.0014
15	WTZR	12.8789	49.1442	68	1992.67	2004.29	11.62	0.0144	0.0203	−0.0009
16	ZIMM	7.4653	46.8771	55	1996.73	2004.29	7.56	0.0151	0.0201	−0.0004
17	ZWEN	36.7586	55.6993	39	1997.40	2004.29	6.88	0.0107	0.0229	−0.0029

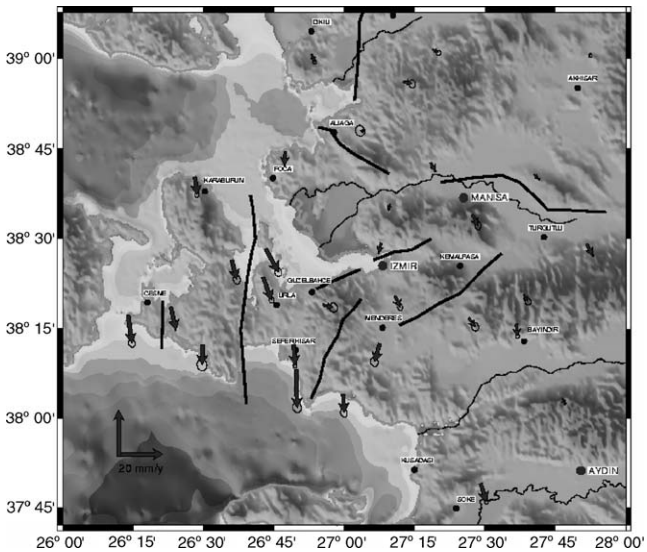

Fig. 4. Horizontal velocity field in ITRF2000 (ellipses are at 95% confidence level). The reference frames for coordinates and velocities was defined by using 17 IGS stations with coordinates and velocities in ITRF2000.

rigid-body rotation was taken from Aktuğ and Kılıçoğlu (2005) and given in Table 4. Selection of sites in defining an Anatolia-fixed frame in Aktuğ and Kılıçoğlu (2005) was based on strain analysis and residual velocities of 68 sites. Details can be found therein. Anatolia–Eurasia pole given by McClusky et al. (2000) is similar. It is considered that even there exist differences in determination of Euler pole due to the correlation of pole location and rate; it has negligible effect on regional velocities. Velocities with respect to Anatolia are shown in Fig. 5b.

4. Strain analysis and relative velocities

Velocity fields of İzmir and surrounding regions were smoothed through a kriging algorithm with a linear variogram model. Efficiency of smoothing velocities is discussed in Ayhan et al. (2002b). Comparison of observed versus smoothed velocities exhibits good agreement as shown in Table 5 and Fig. 6.

Table 3
Horizontal velocities and corresponding 1σ errors in ITRF2000 frame

No.	Site	Longitude (°)	Latitude (°)	v_E (mm/year)	v_N (mm/year)	σ_{v_E} (mm/year)	σ_{v_N} (mm/year)	$\rho_{v_E v_N}$
1	AKCP	27.8630	38.4850	2.6	−5.0	0.1	0.2	−0.10
2	AKGA	27.8730	39.0060	0.2	0.2	0.3	0.3	0.00
3	ARMT	26.7120	38.3930	3.8	−9.7	0.5	0.6	−0.13
4	AVCI	27.5660	37.6950	2.4	−10.2	0.2	0.2	−0.06
5	AYKA	26.7000	39.3110	1.3	−0.8	0.2	0.2	−0.15
6	BAYO	27.3080	38.7110	2.0	−3.8	0.1	0.1	−0.12
7	BIST	27.1810	38.3420	2.3	−4.9	0.5	0.6	−0.16
8	BLKV	26.6010	38.4400	2.2	−8.5	0.7	0.8	−0.16
9	CAKI	27.8130	37.6980	1.5	−9.2	0.2	0.2	−0.06
10	CALI	27.6390	38.3460	1.8	−3.0	0.5	0.7	−0.22
11	CEIL	26.3850	38.3110	2.2	−10.1	0.1	0.1	−0.13
12	CKOY	26.2330	38.2880	1.7	−12.2	0.6	0.7	−0.14
13	DBEY	26.8300	38.1370	0.4	−16.7	0.8	0.9	−0.11
14	DIKI	26.8850	39.0100	1.3	−3.3	0.3	0.4	−0.03
15	DOGA	27.1810	37.6270	4.9	−11.9	0.2	0.2	−0.06
16	GMDR	26.9970	38.0680	0.4	−8.3	0.6	0.7	−0.15
17	GOKT	27.1650	38.5970	−0.9	−2.4	0.2	0.2	−0.04
18	HALP	27.6750	38.6770	2.1	−1.8	0.1	0.2	−0.07
19	KABU	26.4700	38.6710	1.0	−7.8	0.4	0.4	−0.07
20	KINI	27.3160	39.0240	2.3	−1.5	0.4	0.5	−0.04
21	KKLR	27.4430	38.2800	2.8	−3.8	0.6	0.8	−0.14
22	KMLP	27.3570	38.3880	12.9	−6.0	2.8	3.2	−0.12
23	KNRL	27.1270	38.2090	−2.4	−8.0	0.7	0.8	−0.13
24	KOB1	27.1120	39.2440	1.2	−1.1	1.2	0.8	0.17
25	MNSA	27.4550	38.5670	2.5	−4.8	0.6	0.7	−0.17
26	PAYM	26.9260	38.3170	4.5	−1.2	0.7	0.8	−0.06
27	SFRH	26.8210	38.2070	0.6	−9.2	0.3	0.4	−0.06
28	SOKE	27.4860	37.8180	2.5	−8.0	0.4	0.4	−0.06
29	TIRE	27.7760	38.0560	1.1	−2.4	0.2	0.2	−0.06
30	UADA	26.7220	38.4720	5.4	−10.2	0.6	0.8	−0.14
31	UCTP	27.6130	38.2630	0.4	−5.2	0.4	0.4	−0.01
32	YAMA	27.1310	38.4880	−1.0	−4.5	0.1	0.1	−0.11
33	YENF	26.7910	38.7410	−0.2	−5.9	0.1	0.1	−0.14
34	YKOY	27.0730	38.7980	−2.0	0.2	0.8	1.0	−0.12
35	YUNT	27.2110	38.9350	3.9	−1.0	0.6	0.7	−0.14
36	ZEYT	26.4970	38.2050	−0.2	−8.7	0.9	1.0	−0.06

Table 4
Euler poles of rotation used in regional reference Frame Definition (Aktuğ and Kılıçoğlu, 2005)

Model	Φ (°)	λ (°)	Ω (°/Ma)
Eurasia–ITRF2000	56.2 ± 0.3	258.6 ± 0.5	0.253 ± 0.001
Anatolia–Eurasia	31.68 ± 0.06	31.83 ± 0.03	1.447 ± 0.01

Table 5
Residuals statistics between observed and smoothed velocities

	v_{EAST} (mm)	v_{NORTH} (mm)
Minimum	−0.7	−1.4
Maximum	3.0	3.8
Mean	0.4	0.1
Median	0.1	0.1
RMS	0.9	1.0

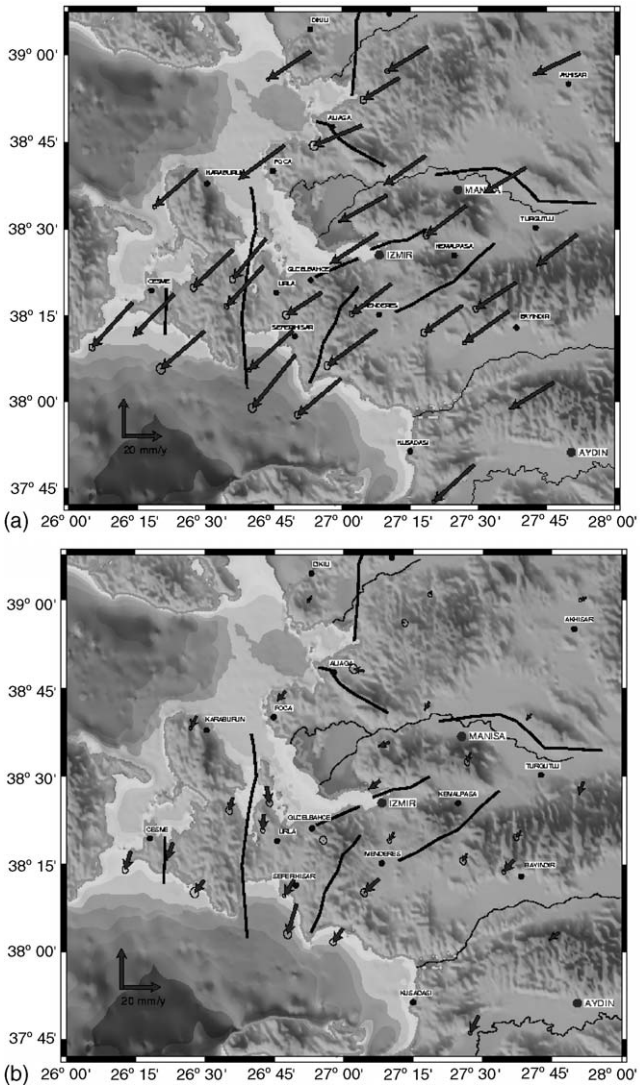

Fig. 5. Horizontal velocity field in: (a) Eurasia-fixed frame and (b) Anatolia-fixed frame (ellipses are at 95% confidence level).

For computation of strain parameters, observed velocities were decomposed into three parts as strain tensor, rotation tensor and translation as given in Feigl et al. (1990) and Demir (1999). All parameters were obtained at $8' \times 8'$ grid nodes through least-squares adjustment using the method given in Shen et al. (1996).

Principal strain rates and directions were computed through eigen analysis of strain rate tensor (Turcotte and Schubert, 1982) and given in Fig. 7 and Table 6. Rotation and shear strain rates computed for the region are given in Figs. 8 and 9, respectively.

In addition to strain analysis, which is independent from frame definition, relative velocities were produced for İzmir Bay and Karaburun Peninsula. Relative velocities of sites in the west of Karaburun-Gülbahçe fault line with respect to an average velocity of two sites lying in the east are shown in Fig. 10. Similarly, relative velocities of sites in the peninsula with respect to an average velocity of four sites lying in the northeast of the peninsula are shown in Fig. 11.

5. Results and discussion

In this study, contemporary velocities of a concentrated monitoring network in İzmir and surrounding regions were analyzed in terms of crustal deformation. Nevertheless, due to the fact that GPS observations are confined to land, GPS

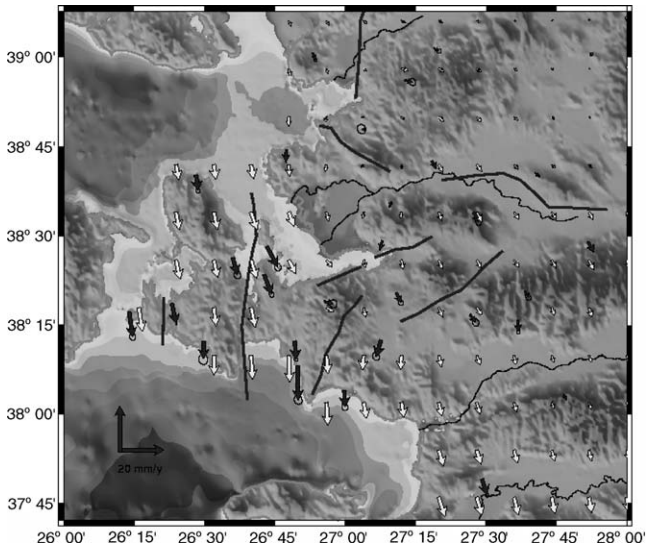

Fig. 6. Smoothed and observed velocities in ITRF2000. Black arrows show observed velocities while white ones show smoothed velocities at grid points.

results can partly show tectonic mechanisms in the region. Combination of daily solutions revealed a good precision with daily repeatabilities of 1–4 mm and 5–8 mm for horizontal and heights, respectively. We are not aware of any site digressing from assumed linear velocity model under a non-tectonic local effect. We computed with respect to ITRF2000, Eurasia-fixed frame and Anatolia-fixed frame alternatively. Post-fit RMS of 17 stations was found to be 1.8 mm and 0.4 mm/year for coordinates and velocities, respectively.

Since the computed velocities are dependent on the datum (reference frame) defined, we computed the strain field parameters. Maximum and minimum extension rates confirm the extension of İzmir Bay in consistent with Western Anatolia. However, relative velocity field shows that extension of İzmir Bay is higher and gradually increasing to the west. To form an analogy, westward increasing extension of İzmir Bay can be thought of a wedge with the origin at the east of İzmir Bay. Another obvious indication of this wedge-like extension is the clockwise rotation of Karaburun Peninsula. These major characteristics of İzmir Bay and Karaburun Peninsula apparently govern the overall tectonic

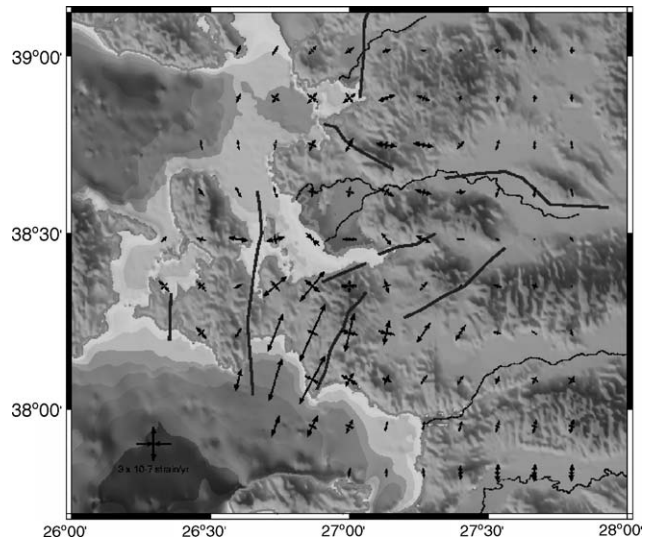

Fig. 7. Principal strain rates (ε_1 and ε_2). Arrows directed outside and inside indicate maximum extension and compression respectively in 10^{-7} strain/year.

Table 6
Principal strains computed at grid nodes

Latitude (°)	Longitude (°)	ε_{max} (10^{-7} year^{-1})	$\sigma_{\varepsilon_{max}}$ (10^{-7} year^{-1})	ε_{min} (10^{-7} year^{-1})	$\sigma_{\varepsilon_{min}}$ (10^{-7} year^{-1})	Latitude (°)	Longitude (°)	ε_{max} (10^{-7} year^{-1})	$\sigma_{\varepsilon_{max}}$ (10^{-7} year^{-1})	ε_{min} (10^{-7} year^{-1})	$\sigma_{\varepsilon_{min}}$ (10^{-7} year^{-1})
37.950	26.733	0.78	0.353	−0.48	0.288	38.483	27.133	2.26	0.552	0.98	0.210
37.950	26.867	1.00	0.356	−0.46	0.373	38.483	27.267	2.00	0.343	0.74	0.153
37.950	27.000	0.95	0.289	−0.3	0.358	38.483	27.400	0.90	0.144	0.24	0.215
37.950	27.133	0.82	0.174	−0.17	0.237	38.483	27.533	0.66	0.185	0.28	0.128
37.950	27.267	0.94	0.169	−0.18	0.162	38.483	27.667	0.86	0.143	0.29	0.182
37.950	27.400	1.26	0.148	−0.3	0.171	38.483	27.800	0.92	0.118	0.2	0.218
37.950	27.533	1.49	0.121	−0.41	0.199	38.617	26.467	0.56	0.180	−0.1	0.190
37.950	27.667	1.59	0.092	−0.42	0.186	38.617	26.600	0.76	0.246	−0.09	0.165
37.950	27.800	1.60	0.082	−0.42	0.193	38.617	26.733	0.66	0.206	−0.56	0.198
38.083	26.600	1.83	0.878	−0.36	0.200	38.617	26.867	0.75	0.243	−0.65	0.119
38.083	26.733	3.58	0.933	−0.29	0.304	38.617	27.000	0.94	0.161	−0.43	0.084
38.083	26.867	4.83	1.027	−1.08	0.513	38.617	27.133	0.97	0.153	0.32	0.208
38.083	27.000	1.23	0.601	−0.96	0.421	38.617	27.267	2.01	0.389	0.65	0.104
38.083	27.133	0.89	0.383	−0.41	0.442	38.617	27.400	0.85	0.117	−0.53	0.200
38.083	27.267	0.92	0.304	0.16	0.229	38.617	27.533	1.03	0.234	0.01	0.107
38.083	27.400	0.90	0.236	−0.15	0.182	38.617	27.667	1.69	0.207	0.1	0.121
38.083	27.533	0.93	0.219	−0.57	0.210	38.617	27.800	1.38	0.175	0.15	0.161
38.083	27.667	1.03	0.226	−0.69	0.227	38.750	26.467	0.56	0.203	−0.29	0.187
38.083	27.800	0.87	0.219	−0.43	0.252	38.750	26.600	0.60	0.273	−0.32	0.192
38.217	26.467	0.87	0.651	−1.17	0.510	38.750	26.733	0.66	0.275	−0.4	0.210
38.217	26.600	1.02	0.539	−0.64	0.301	38.750	26.867	0.96	0.267	−0.38	0.139
38.217	26.733	2.73	0.657	−0.41	0.322	38.750	27.000	0.97	0.178	−0.5	0.144
38.217	26.867	3.99	0.525	−0.78	0.525	38.750	27.133	0.99	0.135	−0.41	0.211
38.217	27.000	1.95	0.399	−0.96	0.370	38.750	27.267	1.06	0.229	0.19	0.283
38.217	27.133	1.22	0.338	−0.36	0.508	38.750	27.400	0.83	0.175	−0.69	0.222
38.217	27.267	1.18	0.369	0.42	0.288	38.750	27.533	0.83	0.252	−0.17	0.138
38.217	27.400	0.43	0.510	0.04	0.204	38.750	27.667	1.09	0.184	0.01	0.088
38.217	27.533	−0.26	0.403	−0.54	0.306	38.750	27.800	1.04	0.117	−0.06	0.112
38.217	27.667	0.51	0.268	−0.65	0.150	38.883	26.600	0.90	0.145	−0.41	0.193
38.217	27.800	0.60	0.236	−0.63	0.134	38.883	26.733	1.01	0.157	−0.31	0.216
38.350	26.333	0.79	0.473	−0.66	0.761	38.883	26.867	1.11	0.154	−0.22	0.193
38.350	26.467	0.61	0.428	−0.64	0.796	38.883	27.000	1.13	0.165	−0.07	0.151
38.350	26.600	0.69	0.306	−0.44	0.498	38.883	27.133	1.13	0.229	0.24	0.177
38.350	26.733	1.16	0.389	−0.93	0.309	38.883	27.267	0.68	0.185	0.64	0.339
38.350	26.867	0.67	0.279	−1.76	0.346	38.883	27.400	0.83	0.185	−0.07	0.159
38.350	27.000	0.57	0.442	−0.86	0.316	38.883	27.533	0.61	0.169	−0.14	0.108
38.350	27.133	1.22	0.464	−0.19	0.507	38.883	27.667	0.54	0.129	−0.08	0.095
38.350	27.267	0.83	0.290	0.58	0.400	38.883	27.800	0.70	0.108	−0.09	0.103
38.350	27.400	0.43	0.234	0.14	0.421	39.017	26.600	0.99	0.128	−0.07	0.196
38.350	27.533	0.31	0.338	−0.06	0.311	39.017	26.733	1.05	0.154	0.13	0.199
38.350	27.667	0.28	0.250	0.06	0.331	39.017	26.867	1.09	0.157	0.14	0.191
38.350	27.800	0.51	0.231	−0.18	0.130	39.017	27.000	1.06	0.179	0.07	0.185
38.483	26.333	0.49	0.206	0.35	0.387	39.017	27.133	0.87	0.248	0.12	0.208
38.483	26.467	0.78	0.367	0.4	0.189	39.017	27.267	0.68	0.244	0.14	0.300
38.483	26.600	1.26	0.384	0.37	0.205	39.017	27.400	0.70	0.181	−0.21	0.209
38.483	26.733	0.69	0.322	−0.24	0.419	39.017	27.533	0.57	0.149	−0.28	0.123
38.483	26.867	0.54	0.236	−1.13	0.149	39.017	27.667	0.50	0.133	−0.22	0.113
38.483	27.000	0.75	0.249	−0.84	0.244	39.017	27.800	0.58	0.120	−0.15	0.112

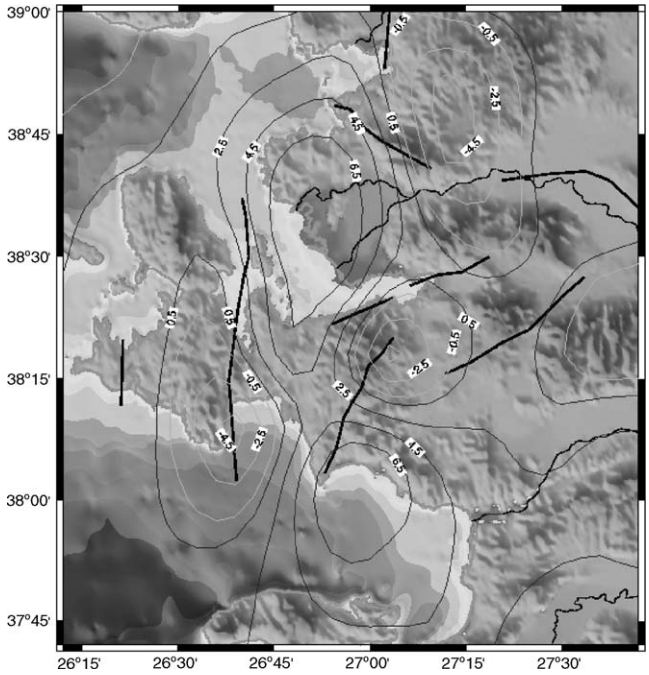

Fig. 8. Rigid-body rotation rates (w) in degrees/million year (positive values indicate a counter clockwise rotation).

regime in İzmir and surrounding regions. Results show east–west shortening between Karaburun Peninsula and northern part of İzmir Bay together and extension of İzmir Bay. Differential motion driven by this rotation and extension is considered to be accommodated by geologically distinct Urla Block in the middle bounded by associated strike–slip faulting. Shear strain rates in the area with negative values can be thought of as another indication of NW–SE extension.

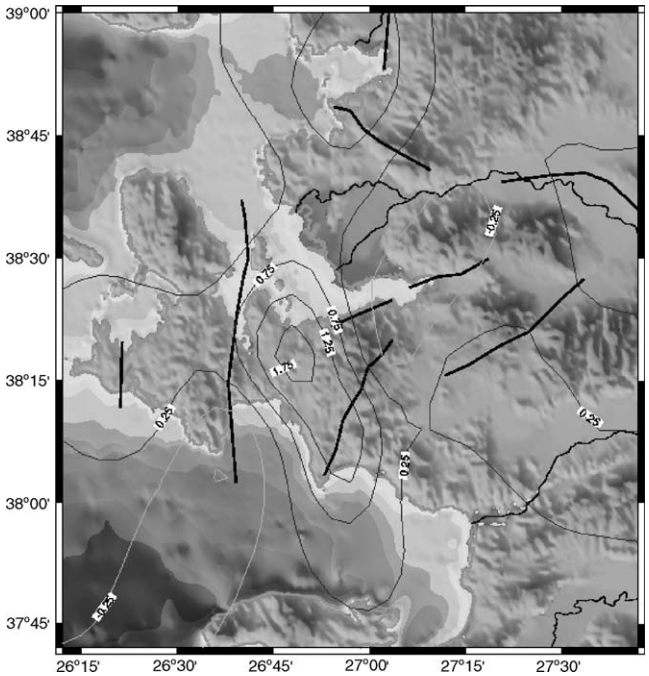

Fig. 9. Shear rates (ε_{xy}) in 10^{-7} strain/year (positive values indicate a right-lateral shear, whereas negative values show shear in left-lateral sense).

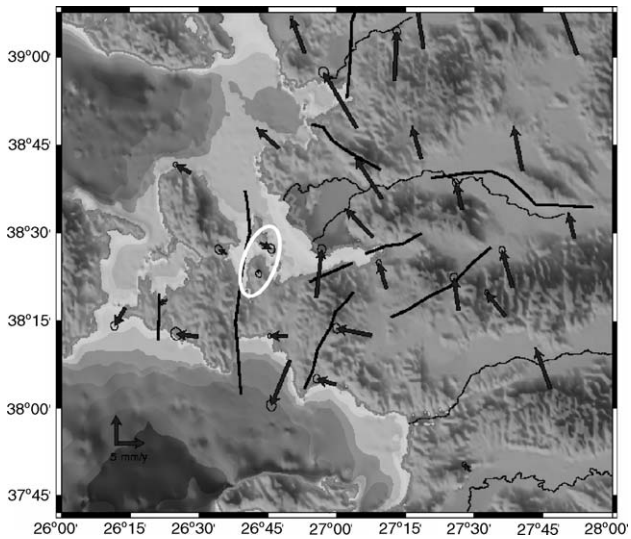

Fig. 10. Relative velocities of GPS stations with respect to an average velocity of Uzunada and Armutalan sites (circumscribed by white ellipse) located in the east of Gülbahçe-Karaburun Fault (error ellipses drawn at 95% confidence level).

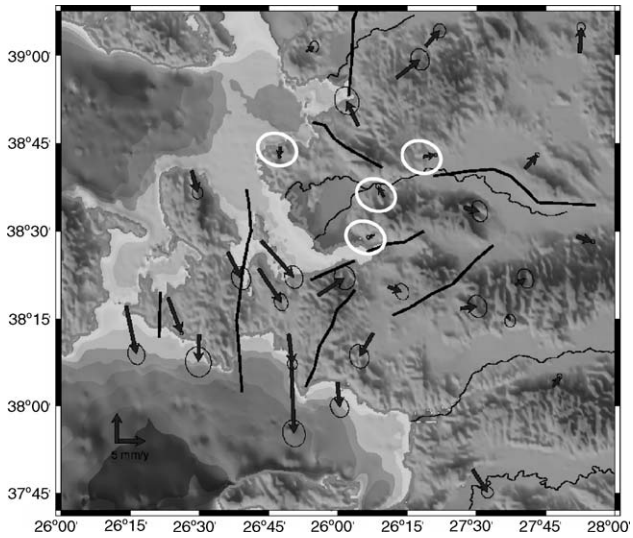

Fig. 11. Relative velocities of GPS stations with respect to an average velocity of Yeni Foça, Yamanlar, Göktepe and Bağ Yolu sites (circumscribed by white ellipse) located in the northeast of İzmir Bay (error ellipses drawn at 95% confidence level).

In this aspect, the part of peninsula to the west of Gülbahçe-Karaburun Fault exhibits an east–west shortening and north–south extension regime with respect to northeast of İzmir Bay in accordance with a right-lateral faulting and a clockwise rotation. Besides, differential motion between Karaburun and Foça shows that right-lateral faulting of Gülbahçe-Karaburun Fault continues northward passing the virtual line connecting Karaburun and Foça.

6. Conclusions

Extensional shear rates along the northern and southern parts of Tuzla Fault can be considered a right-lateral faulting with a thrusting component in the south. Extensional rate along Tuzla Fault is maximum in the region and confirms its active state.

Part of the peninsula comprising of Dikmen mountain and geologically distinct Urla Block between Gülbahçe-Karaburun Fault and Dikmen Mountain is bounded by two right-lateral faults, namely Gülbahçe-Karaburun Fault to the west and Tuzla Fault to the east. The differential motion arising from two right-lateral systems needs to be absorbed by either rotation of this block or a left lateral fault system between Urla Block and Dikmen Mountain. Since no significant rotation was observed for the block between Gülbahçe-Karaburun and Tuzla Faults, this differential motion is attributed to the existence of a left-lateral active Urla Fault between Urla Block and Dikmen Mountain. Westernmost part of Karaburun Peninsula appears to move relative to the peninsula implying strike–slip faulting, but more GPS data are required to verify this relatively small scale process.

Urla Block bounded by Gülbahçe-Karaburun Fault to the west and Dikmen Mountain to the east appears to have a relative motion with respect to the northeastern part of İzmir Bay. The differential motion observed was at a rate of 3–5 mm/year and 5–6 mm/year to the east and south, respectively, for the block between Gülbahçe-Karaburun and Tuzla Faults.

Neotectonic regime in İzmir Bay and surrounding regions can be considered to be dominated by southern motion of Urla Block and corresponding east–west shortening between Karaburun Peninsula and northern part of İzmir Bay which is apparently under an extension regime gradually increasing to the west.

As is in Western Anatolia, north–south extension is dominant in almost all parts of the region despite the fact that they exhibit significantly higher rates in the middle of the peninsula. Extensional rates along Tuzla Fault lying nearly perpendicular to İzmir Bay and in its west are maximum in the region with an extension rate of $300–500 \pm 80–100$ nanostrain/year and confirm its active state. Extensional rates in other parts of the region are at level of 50–150 nanostrain/year as expected in the other parts of Western Anatolia.

References

Akıncı, A., Eyidoğan, H., Göktürkler, G., Akyol, N., Ankaya, O., 2000. Investigation of seismicity and earthquake hazard in İzmir and surroundings. In: Symposium on Seismicity of Western Turkey, Izmit, Turkey, 24–27 May.

Aktuğ, B., 2003. Velocity field of ITRF and a look at relative velocity frames. Harita Dergisi (J. Mapping) 130, 12–31, Ankara (in Turkish).

Aktuğ, B., 2004. Data reduction methods in modern geodesy and constraints handling. Harita Dergisi (J. Mapping) 131, 1–19, Ankara (in Turkish).

Aktuğ, B., Kılıçoğlu, A., 2005. Establishing regional reference frames for determining active deformation areas in Anatolia. In: IAG-IABO-IAPSO Joint Assembly, Cairns, Australia, 22–26 September.

Altamimi, Z., Sillard, P., Boucher, C., 2002. ITRF2000: a new release of the International Terrestrial Reference Frame for Earth science applications. J. Geophys. Res. 107 (B10), 2214.

Altiner, Y., Becker, M., Franke, P., Hoppe, W., Müller, W., Schlüter, W., Seeger, H., 1994. GPS-geodynamic-projects of IfAG in Europe. In: Proceedings of the 1st Turkish International Symposium on Deformations, Istanbul, September 5–9.

Aydan, Ö., Kumsar, H., Ulusay, R., 2000. An approach the seismicity of Western Anatolia through GPS measurements. In: Symposium on Seismicity of Western Turkey, Izmit, Turkey, 24–27 May.

Ayhan, M.E., Demir, C., Lenk, O., Kılıçoğlu, A., Aktuğ, B., Açıkgöz, M., Fırat, O., Şengün, Y.S., Cingöz, A., Gürdal, M.A., Kurt, A.İ., Ocak, M., Türkezer, A., Yıldız, H., Bayazıt, N., Ata, M., Çağlar, Y., Özerkan, A., 2002a. Turkish National Fundamental GPS Network-1999A (TNFGN-99A). Harita Dergisi (J. Mapping) (16), Ankara (in Turkish) (special issue).

Ayhan, M.E., Demir, C., Lenk, O., Kilicoglu, A., Altiner, Y., Barka, A.A., Ergintav, S., Özener, H., 2002b. Interseismic strain accumulation in the Marmara Sea region. Bull. Seismol. Soc. Am. 92, 216–229.

Ayhan, M.E., Aktuğ, B., Acıkgöz, M., Demir, C., Lenk, O., Reilinger, R.E., 2003. Contemporary crustal deformation in Turkey constrained by GPS measurements between 1992 and 2002. In: Int. Workshop on the North Anatolian, East Anatolian and Dead Sea Fault Systems: Recent Progress in Tectonics and Paleoseismology, 31 August–12 September. METU, Ankara, Turkey.

Brockmann, E., 1996. Combination of solutions for geodetic and geodynamic applications of the global positioning system (GPS). Ph.D. Dissertation. Astronomical Institute, University of Berne, Switzerland.

Demir, C., 1999. Investigation of horizontal crustal motion and strain accumulation in western part of North Anatolian Fault. Ph.D. Dissertation. Yıldız Technical University, İstanbul.

Dong, D., Herring, T.A., King, R.W., 1998. Estimating regional deformation from a combination of space and terrestrial data. J. Geodyn. 72, 200–211.

Emre, Ö., Barka, A., 2000. Active faults between Gediz Graben and Agean Sea (İzmir region). In: Symposium on Seismicity of Western Turkey, Izmit, Turkey, 24–27 May, pp. 131–132.

Erdik, M., Ansal, A., Aydınoğlu, N., Barka, A., Işıkara, M.A., Yüzgüllü, Ö., Avcı, J., Biro, Y., Birgören, G., 1999. İzmir Earthquake Scenario and Master Plan., http://www.izmir-bld.gov.tr/izmirdeprem/izmirrapor.htm.

Eyidoğan, H., 1987. Rates of crustal deformation in Western Turkey as deduced from major earthquakes. Tectonophysics 148, 83–92.

Feigl, K.L., King, R.W., Jordan, T.H., 1990. Geodetic measurements of Tectonic Deformation in the Santa Maria Fold and Thrust Belt, California. J. Geophys. Res. 95 (B3), 2679–2699.

Herring, T.A., 1997. GAMIT/GLOBK Kalman Filter VLBI and GPS Analysis Program; Version 4.1. Massachusetts Institute of Technology, Cambridge.

Jackson, J., Haines, J., Holt, W., 1992. The horizontal velocity field in the deforming Aegean Sea Region determined from the moment tensors of earthquakes. J. Geophys. Res. 97 (B12), 17657–17684.

Jackson, J.A., McKenzie, D.P., 1984. Active tectonics of Alpine–Himalayan Belt between western Turkey and Pakistan. Geophys. J. R. Astron. Soc. 77, 185–265.

Kahle, H.-G., Cocard, M., Peter, Y., Geiger, A., Reilinger, R., Barka, A., Veis, G., 2000. GPS-derived strain rate field within the boundary zones of the Eurasian, African, and Arabian plates. J. Geophys. Res. 105 (B10), 23353–23370.

Kahle, H.G., Müller, M.V., Geiger, A., Danuser, G., Mueller, S., Veis, G., Biliris, H., Paradissis, D., 1995. The strain field in NW Greece and the Ionian Islands: results inferred from GPS measurements. Tectonophysics 249, 41–52.

Kahle, H.-G., Straub, C., Reilinger, R., McClusky, S., King, R., Hurst, K., Veis, G., Kastens, K., Cross, P., 1998. The strain rate field in the eastern Mediterranean region, estimated by repeated GPS measurements. Tectonophysics 294, 237–252.

Kahle, H.-G., Cocard, M., Peter, Y., Geiger, A., Reilinger, R., McClusky, S., King, R., Barka, A., Veis, G., 1999. The GPS strain rate field in the Aegean Sea and Western Anatolia. Geophys. Res. Lett. 26, 2513–2516.

Kılıçoğlu, A., 1999. Combination of GPS measurements and investigation of results for crustal deformation for İTU-ETHZ-TUJJB GPS Project. Ph.D. Dissertation. ITU, İstanbul.

Kissel, C., Laj, C., Şengör, A.M.C., Poisson, A., 1987. Paleomagnetic evidence for rotation in opposite senses of adjacent blocks in northeastern Aegea and Western Anatolia. Geophys. Res. Lett. 14 (September (9)), 907–910.

Lundgren, P., Giardini, D., Russo, M., 1998. A geodynamical framework for eastern Mediterranean kinematics. Geophys. Res. Lett. 25 (November (21)), 4007–4010.

McClusky, S., Balasdsanian, S., Barka, A., Demir, C., Georgiev, I., Hamburger, M., Hurst, K., Kastens, K., Kekelidze, G., Kotzev, R.K.V., Lenk, O., Mahmoud, S., Mishin, A., Nadariya, M., Ouzounis, A., Paradissis, D., Peter, Y., Prilepin, M., Reilinger, R., Sanli, I., Seeger, H., Tealeb, A., Toksoz, M.N., Veis, G., 2000. Global positioning system constraints on crustal movements and deformations in the eastern Mediterranean and Caucasus. J. Geophys. Res. 105, 5695–5719.

Mervart, L., 1996. Ambiguity resolution techniques in geodetic and geodynamic applications of the GPS. Ph.D. Dissertation. AUIB, Bern.

Nyst, M., Thatcher, W., 2004. New constraints on the active tectonic deformation of the Aegean. J. Geophys. Res. 109, B11406, doi:10.1029/2003JB002830.

Ocakoğlu, N., 2004. Investigation of active tectonics of İzmir Bay and Alaçatı-Doğanbey-Kuşadası offshores through seismic reflection data. Ph.D. Dissertation. İstanbul Technical University.

Orbay, N., Sanver, M., Hisarlı, M., İşseven, T., Özçep, F., 2000. Paleomagnetism and tectonic evolution of Karaburun Peninsula. In: Symposium on Seismicity of Western Turkey, Izmit, Turkey, 24–27 May, pp. 59–67.

Rothacher, M., Mervart, L., 1996. The Bernese GPS Software Version 4.0. Astronomical Institute, University of Berne, Berne, Switzerland.

Shen, Z.-K., Jackson, D.D., Ge, X.B., 1996. Crustal deformation across and beyond the Los Angeles basin from geodetic measurements. J. Geophys. Res. 101, 27957–27980.

Straub, C., Kahle, H.G., 1995. Active crustal deformation in the Marmara Sea Region, NW Anatolia, inferred from GPS measurements. Geophys. Res. Lett. 26, 2513–2516.

Şaroğlu, F., Emre, Ö., Kuşçu, İ., 1992. Turkish Active Faults Map. Directoriate of Mineral Research and Exploration, Ankara, Turkey.

Taymaz, T., Jackson, J., McKenzie, D., 1991. Active tectonics of Alpine–Himalayan Belt between western Turkey and Pakistan. Geophys. J. R. Astron. Soc. 77, 185–265.

Turcotte, D.L., Schubert, G., 1982. Geodynamics: Applications of Continuum Physics to Geological Problems. John Wiley & Sons, New York.

Wessel, P., Smith, W.H.F., 1995. New version of the generic mapping tools released. EOS 76, 329.